Supplementary Materials for manuscript:

Anthocyanin profiling of maize grains using DIESI-MSQD reveals that cyanidin-based derivatives predominate in purple corn, whereas pelargonidin-based molecules occur in red-pink varieties from Mexico

Peniche-Pavía & Tiessen 2020

- Sample information (Table S1-2)
- A visual explanation for the mass methods used (S1),
- Fragmentation patterns for anthocyanin ions (S2-10),
- Extra heatmaps (S11-S12)
- Boxplots for selected anthocyanins (S13-18).

Code	mean ± SD	Code	mean ± SD	Code	mean ± SD
EO1_Pur	0.59 ± 0.03	EO3_Red	0.42 ± 0.02	VM2_Lpu	0.28 ± 0.02
EO1_Red	0.54 ± 0.03	EO3_Lpu	0.48 ± 0.05	VM2_Yew	0.32 ± 0.03
EO1_Lpu	0.59 ± 0.03	EO4_Bro	0.41 ± 0.05	VM3_Pur	0.19 ± 0.01
EO2_Pur	0.50 ± 0.12	EO4_Pur	0.59 ± 0.01	VM3_Lpu	0.20 ± 0.02
EO2_Red	0.53 ± 0.15	EO4_Red	0.59 ± 0.05	VM4_Bla	0.19 ± 0.01
EO2_Lpu	0.54 ± 0.08	CP1_Pur	0.53 ± 0.02	VM4_Pur	0.17 ± 0.02
EO2_Pin	0.58 ± 0.08	CA1_Yew	0.37 ± 0.06	VM4_Bro	0.17 ± 0.02
EO2_Lpi	0.46 ± 0.01	VM1_Pur	0.21 ± 0.02	CN1_Bla	0.51 ± 0.02
EO3_Bro	0.52 ± 0.03	VM2_Bla	0.31 ± 0.03	366_Bla	0.40 ± 0.04
EO3_Pur	0.53 ± 0.04	VM2_Pur	0.31 ± 0.02	ATF_Bla	0.40 ± 0.00

Table S1. Average weights in g of individual kernels. The names of the landraces and Vitamaize entries and the phenotypic color were abbreviated and joined to form a code for subsequent analysis. The first part of the code corresponds to genotype: Elote Occicental (EO), Criollo Amarillo (CA1), Vitamaize (VM), Conico Negro (CN1). The second part of the code corresponds to the kernel color with following abbrViations: purple (Pur), light purple (Lpu), pink (Pin), light pink (Lpi), brown (Bro), yellow (Yew), and black (Bla).

Dry weights in g of individual kernels. Raw data:

Code	Sample I	Sample II	Sample III	Code	Sample I	Sample II	Sample III
EO1_Pur	0.576	0.568	0.626	**CP1_Pur**	0.525	0.507	0.558
EO1_Red	0.543	0.506	0.567	**CA1_Yew**	0.420	0.392	0.297
EO1_Lpu	0.611	0.561	0.588	**VM1_Pur**	0.200	0.200	0.231
EO2_Pur	0.64	0.438	0.418	**VM2_Bla**	0.332	0.283	0.328
EO2_Red	0.384	0.54	0.674	**VM2_Pur**	0.332	0.296	0.302
EO2_Lpu	0.525	0.563	0.544	**VM2_Lpu**	0.301	0.273	0.26
EO2_Pin	0.63	0.622	0.482	**VM2_Yew**	0.34	0.33	0.284
EO2_Lpi	0.449	0.466	0.457	**VM3_Pur**	0.189	0.191	0.202
EO3_Bro	0.486	0.552	0.519	**VM3_Lpu**	0.172	0.211	0.204
EO3_Pur	0.565	0.492	0.526	**VM4_Bla**	0.182	0.182	0.195
EO3_Red	0.402	0.444	0.403	**VM4_Pur**	0.186	0.151	0.181
EO3_Lpu	0.461	0.445	0.53	**VM4_Bro**	0.181	0.141	0.179
EO4_Bro	0.368	0.471	0.392	**CN1_Bla**	0.522	0.486	0.528
EO4_Pur	0.418	0.407	0.391	**366_Bla**	0.359	0.436	0.403
EO4_Red	0.271	0.346	0.37	**ATF_Bla**	0.403	0.406	0.397

Table S2. List of anthocyanins detected with the Neutral Loss Method (MS2 data).

Molecule	Fragment loss of	Parent ion *m/z*
cyanidin-3-*O*-glucoside	162 Da	449
pelargonidn-3-*O*-glucoside	162 Da	433
peonidin-3-*O*-glucoside	162 Da	463
cyanidin-3-*O*-(6"-malonyl-glucoside)	248 Da	535
pelargonidn-3-*O*-(6"-malonyl-glucoside)	248 Da	519
peonidin-3-*O*-(6"-malonyl-glucoside)	248 Da	549
cyanidin-3-*O*-(6"-succinyl-glucoside)	262 Da	549
pelargonidn-3-*O*-(6"-succinyl-glucoside)	262 Da	533
peonidin-3-*O*-(6"-succinyl-glucoside)	262 Da	563
cyanidin-3-*O*-(dimalonyl-glucoside)	334 Da	619
pelargonidn-3-*O*-(dimalonyl-glucoside)	334 Da	605
peonidin-3-*O*-(dimalonyl-glucoside)	334 Da	635
cyanidin-3-*O*-(malonyl, succinyl-glucoside)	348 Da	635
pelargonidn-3-*O*-(malonyl, succinyl-glucoside)	348 Da	619
peonidin-3-*O*-(malonyl, succinyl-glucoside)	348 Da	649
cyanidin-3-*O*-(disuccinyl-glucoside)	362Da	649
pelargonidn-3-*O*-(disuccinyl-glucoside)	362Da	633
peonidin-3-*O*-(disuccinyl-glucoside)	362Da	663

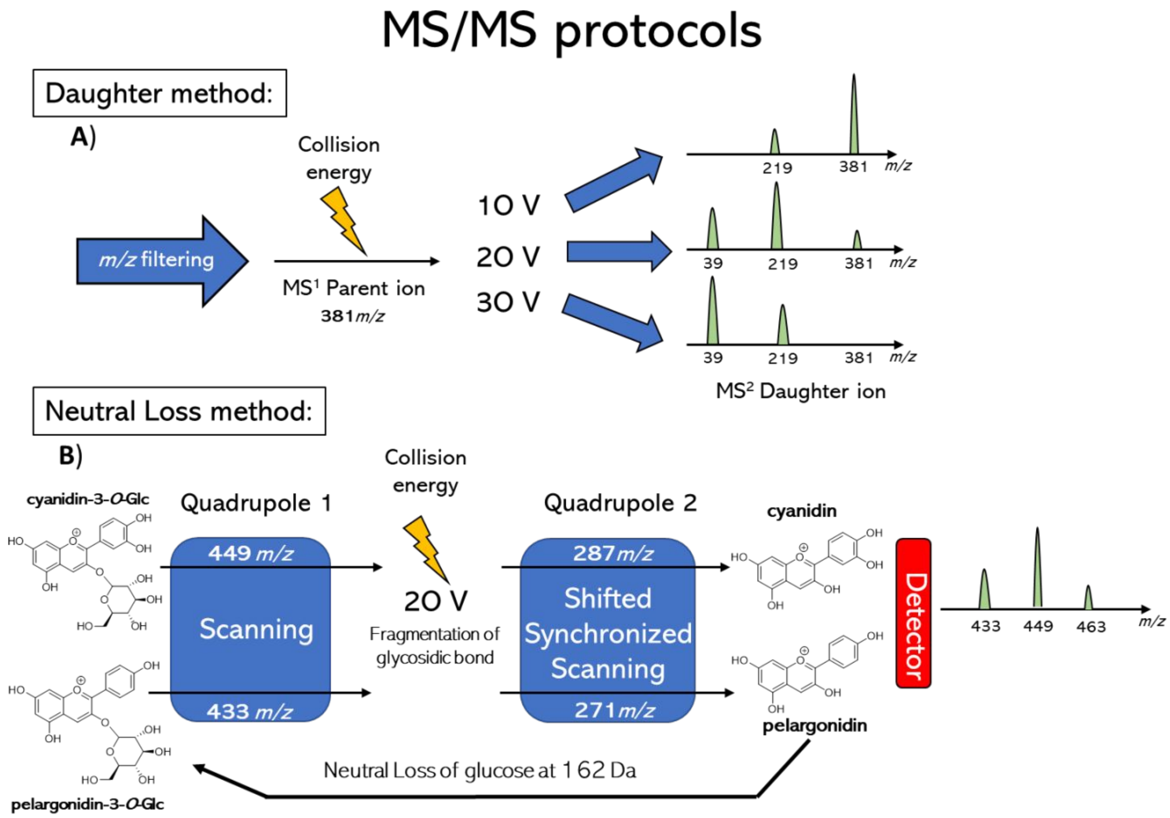

Figure S1. Overview of the two MS/MS methods employed to identify candidate ions. The combination of both methods allowed to tentatively assign ions a chemical structure and thus give them a name.

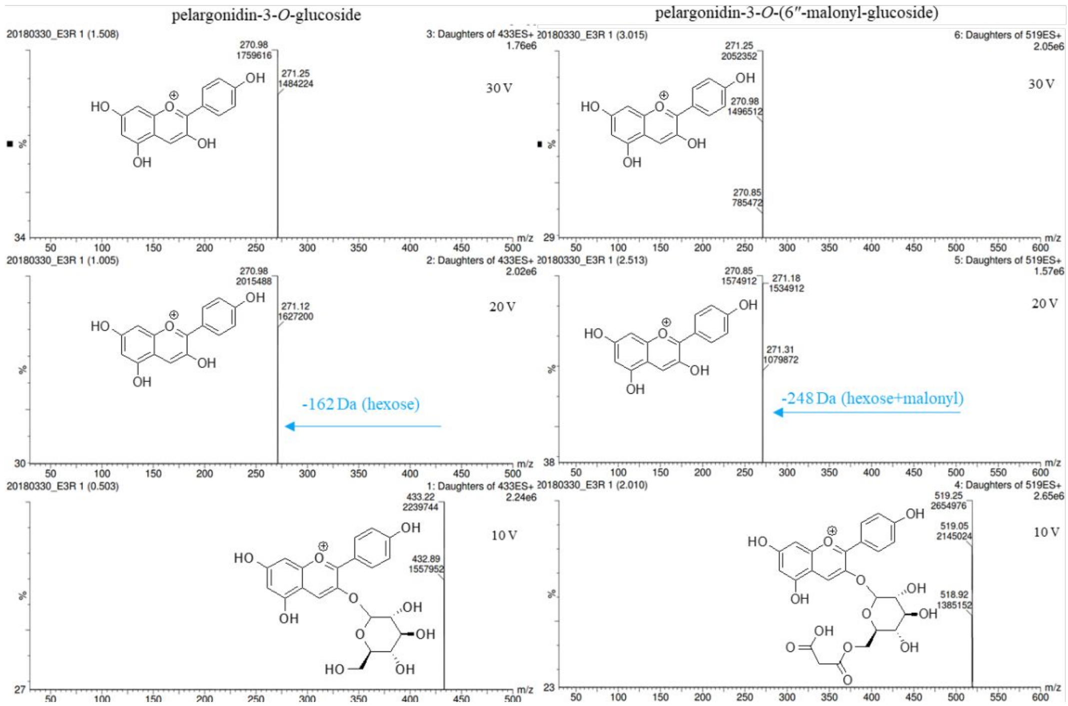

Figure S2. Mass spectra for pelargonidin-3-*O*-glucoside and pelargonidin-3-*O*-(6”-malonyl-glucoside). Data was obtained with Daughters method in MassLynx 4.1 using 10 V, 20 V, and 30 V. Representative data is shown (sample EO3_Red).

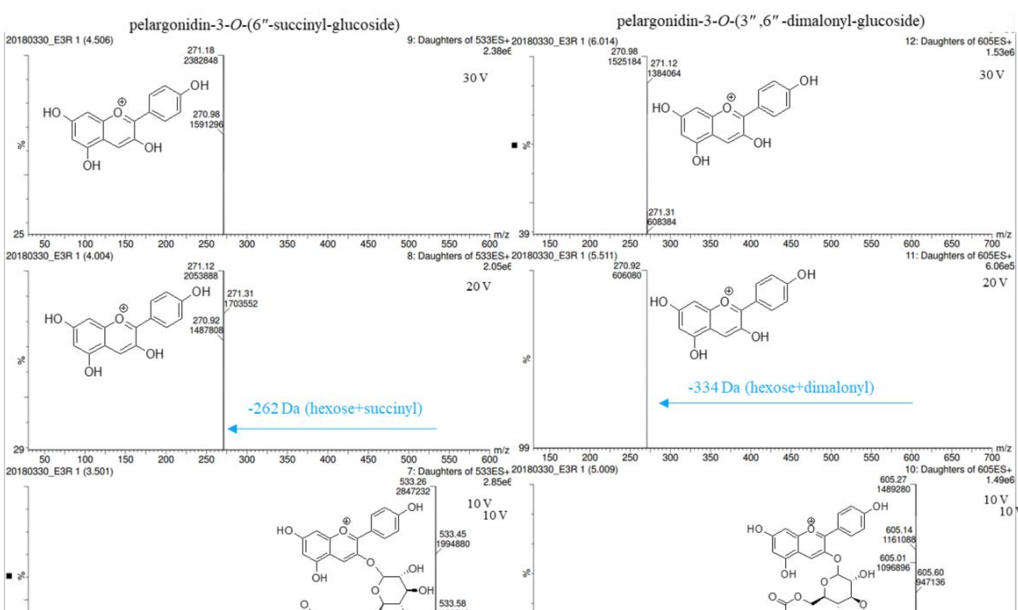

Figure S3. Mass spectra for pelargonidin-3-*O*-(6”-succinyl-glucoside) and pelargonidin-3-*O*-(dimalonyl-glucoside). Data was obtained with Daughters method in MassLynx 4.1 using 10 V, 20 V, and 30 V. Representative data is shown (sample EO3_Red).

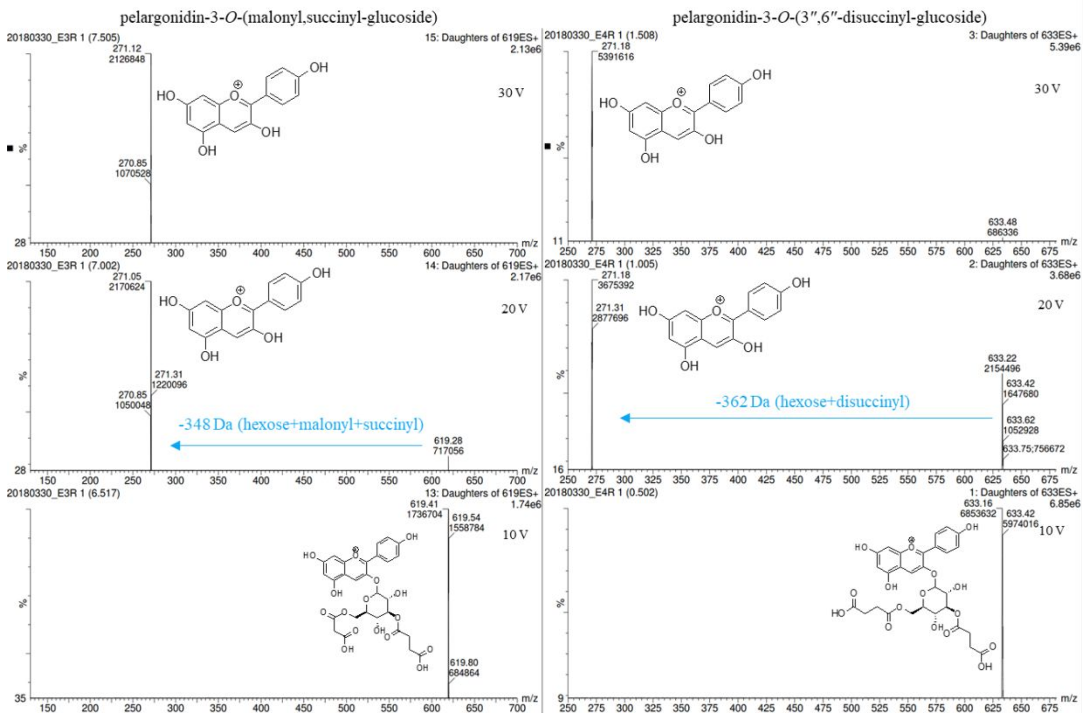

Figure S4. Mass spectra for pelargonidin-3-*O*-(malonyl, succinyl-glucoside) and pelargonidin-3-*O*-(disuccinyl-glucoside). Data was obtained with Daughters method in MassLynx 4.1 using 10 V, 20 V, and 30 V. Representative data is shown (sample EO3_Red).

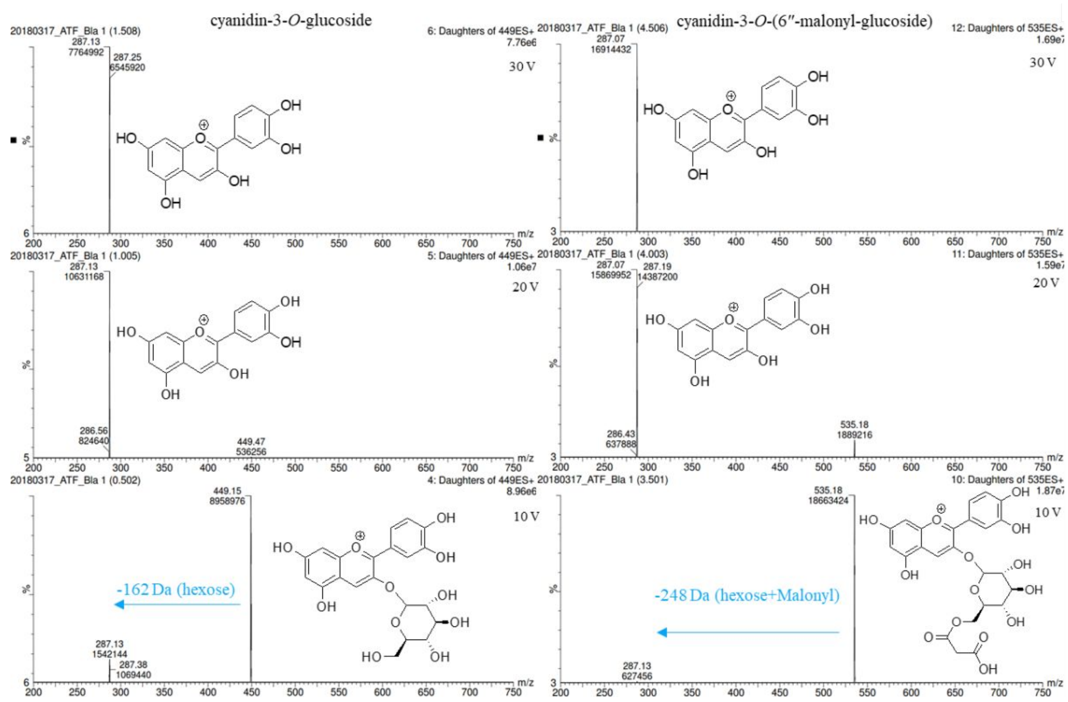

Figure S5. Mass spectra for cyanidin-3-*O*-glucoside and cyanidin-3-*O*-(6”-malonyl-glucoside). Data was obtained with Daughters method in MassLynx 4.1 using 10 V, 20 V, and 30 V. Representative data is shown (sample ATF_Black).

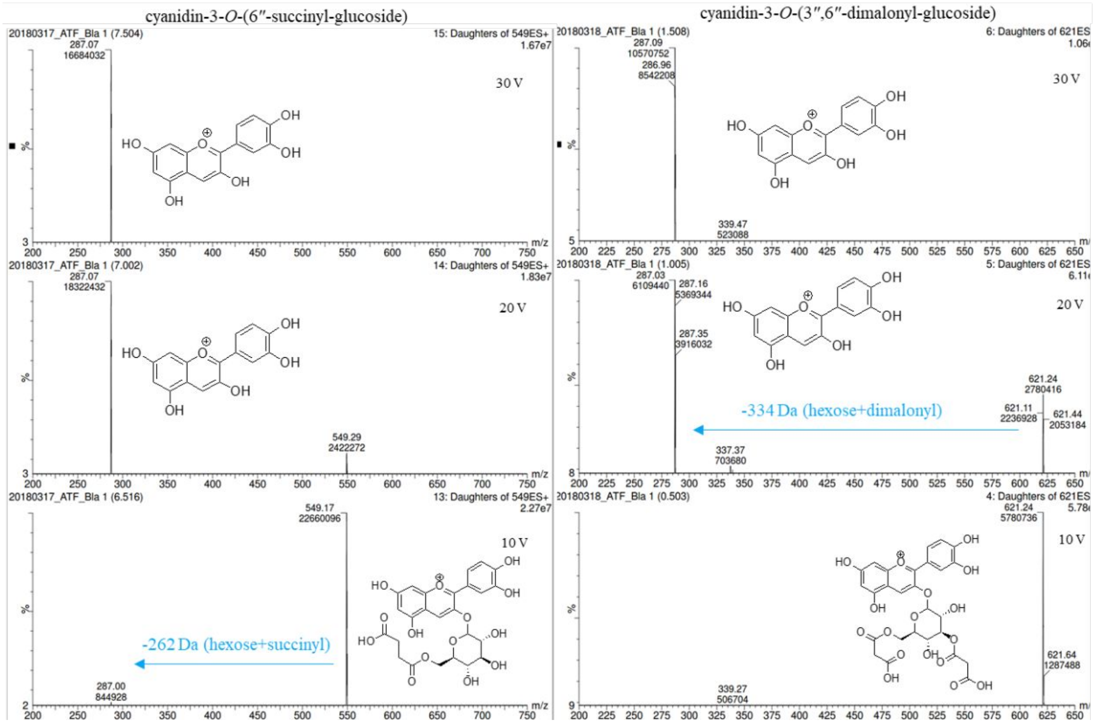

Figure S6. Mass spectra for cyanidin-3(6”-succinyl)-*O*-glucoside and cyanidin-3-*O*-(dimalonyl-glucoside). Data was obtained with Daughters method in MassLynx 4.1 using 10 V, 20 V, and 30 V. Representative data is shown (sample ATF_Black).

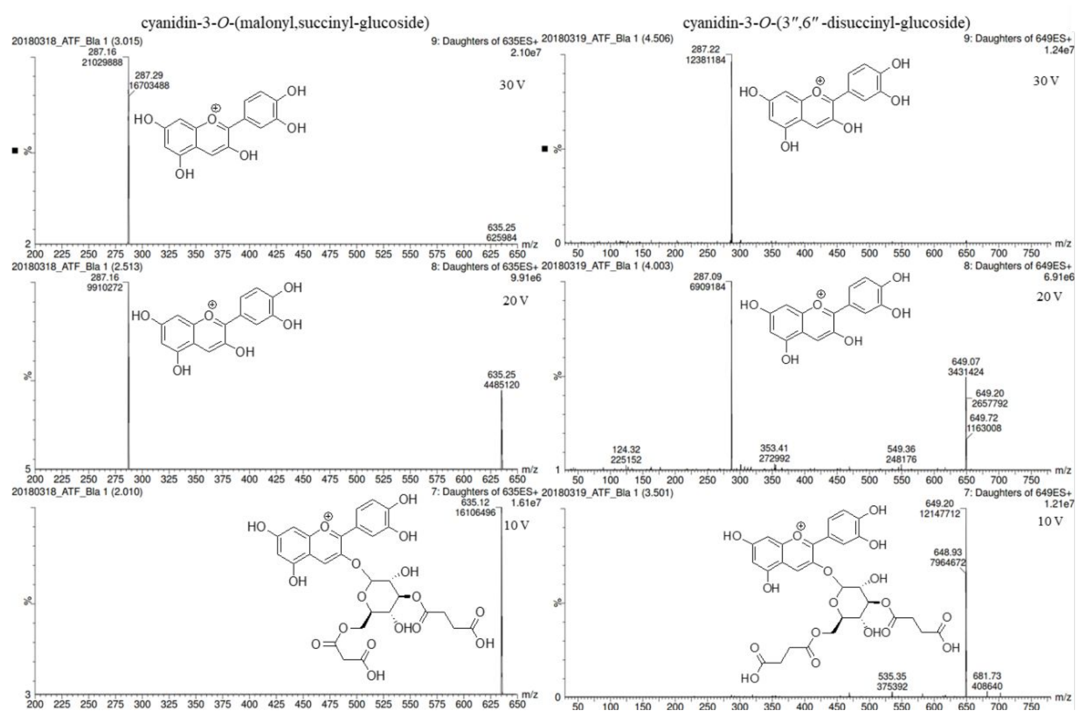

Figure S7. Mass spectra for cyanidin-3-*O*-(malonyl, succinyl-glucoside) and cyanidin-3-*O*-(disuccinyl)-glucoside. Data was obtained with Daughters method in MassLynx 4.1 using 10 V, 20 V, and 30 V. Representative data is shown (sample ATF_Black).

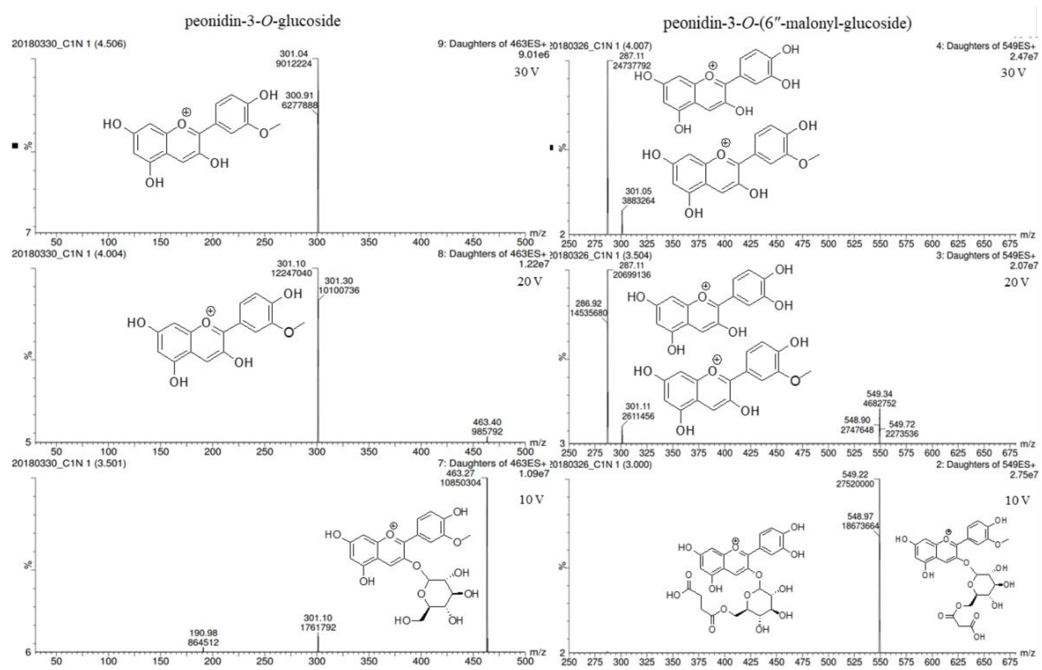

Figure S8. Mass spectra for peonidin-3-*O*-glucoside and peonidin-3-*O*-(6”-malonyl-glucoside) mixed with cyanidn-3-*O*-(6”-succinyl-glucoside). Data was obtained with Daughters method in MassLynx 4.1 using 10 V, 20 V, and 30 V. Representative data is shown (sample CN1_Black).

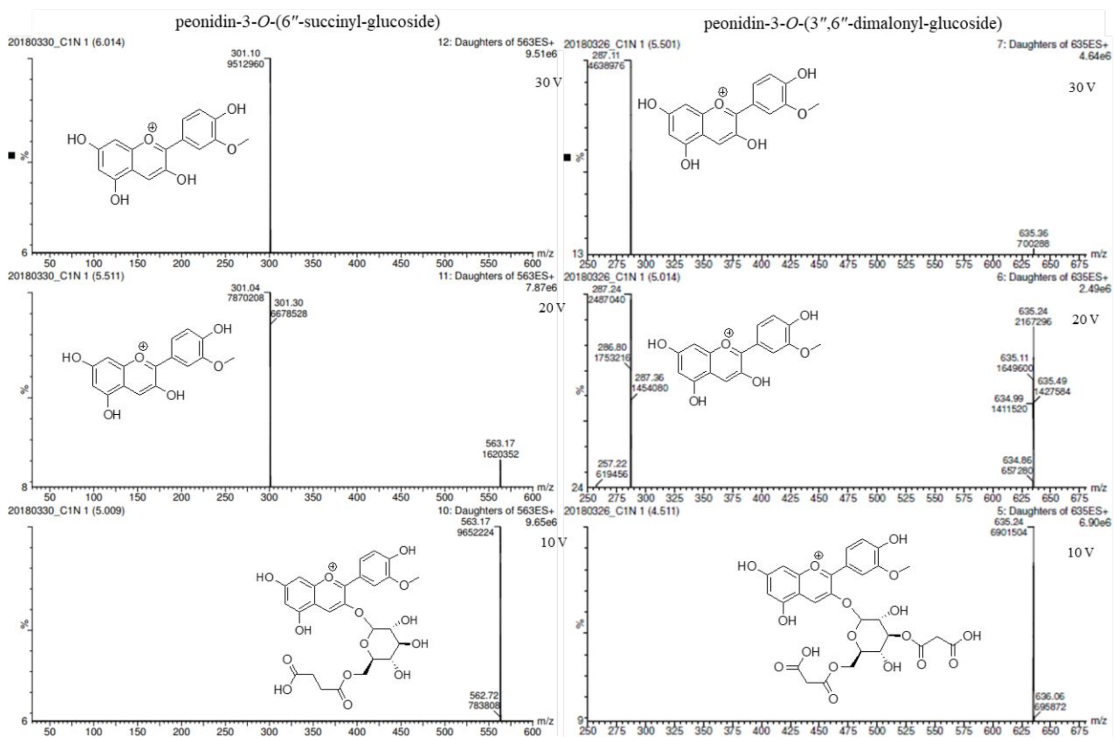

Figure S9. Mass spectra for peonidin-3-*O*-(6”-succinyl-glucoside) and peonidin-3-*O*-(malonyl, succinyl-glucoside) mixed with cyanidin-3-*O*-(disuccinyl-glucoside). Data was obtained with Daughters method in MassLynx 4.1 using 10 V, 20 V, and 30 V. Representative data is shown (sample CN1_Black).

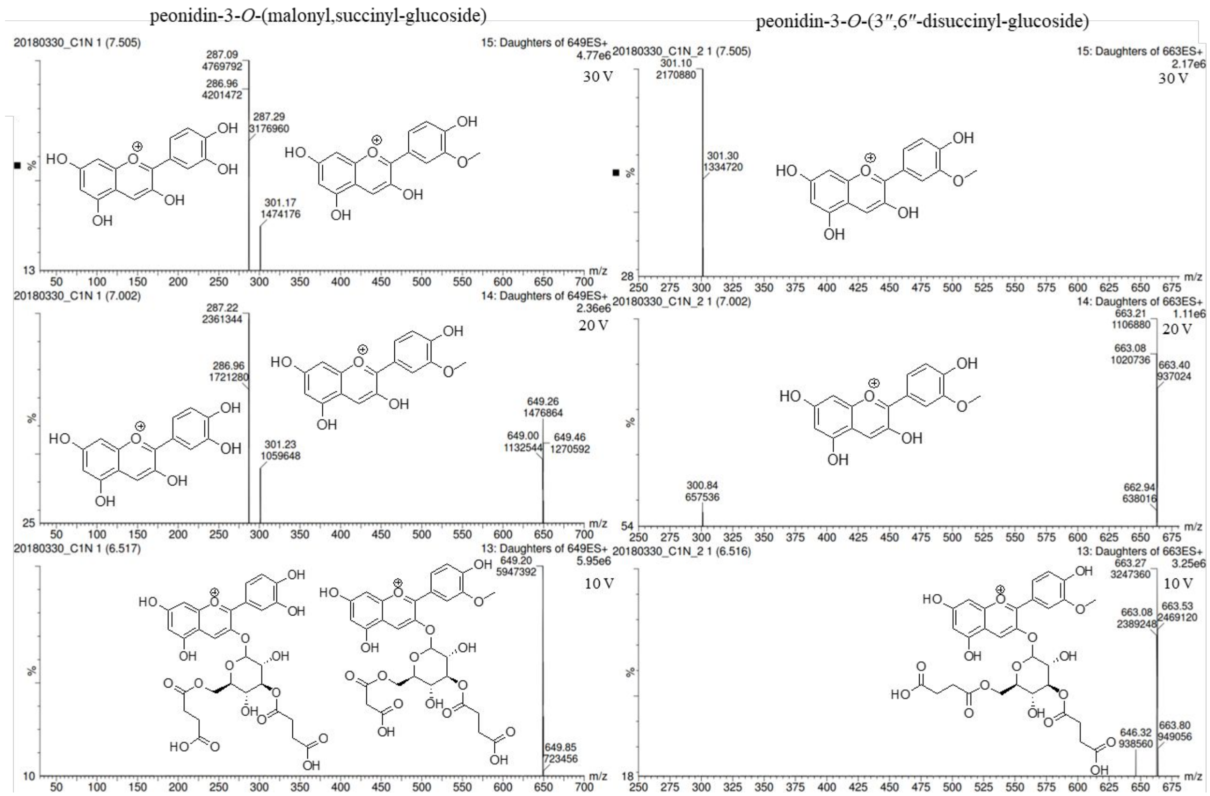

Figure S10. Mass spectra for the presumed peonidin-3-*O*-(malonyl-glucoside) and cyanidin-3-*O*-(disuccinyl-glucoside) and peonidin-3-*O*-(disuccinyl-glucoside) at 649 *m/z* and 663 *m/z*, respectively. The mass spectra were obtained with Daughters method in MassLynx 4.1 using 10 V, 20 V, and 30 V. The sample used was CN1_Black

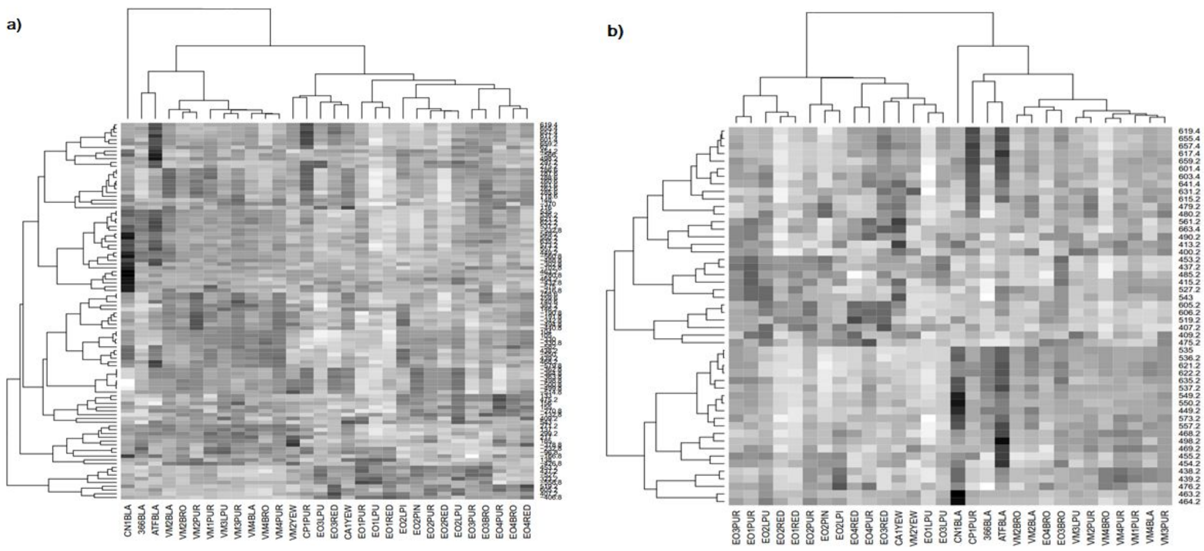

Figure S11. Heat maps using the most significant ions according to their *p*-value for the entry factor in the ANOVA model. In figure a) 100 ions detected in positive and negative ionization mode. It shows three clusters: one for Vitamaize and another one for “Elote occidental” landrace, while “Conico negro” is alone as a third clusted. In Figure b) the hierarchical clustering was done selecting ions only from the range 400-700 m/z. It forms two clusters: one of samples with high anthocyanin concentration which included Vitamaize and brown colored kernels from “Elote occidental”, purple grain from “Pozolero purpura”, and “Conico negro”. The second cluster grouped the rest of the samples: pale, red and purple colored landraces.

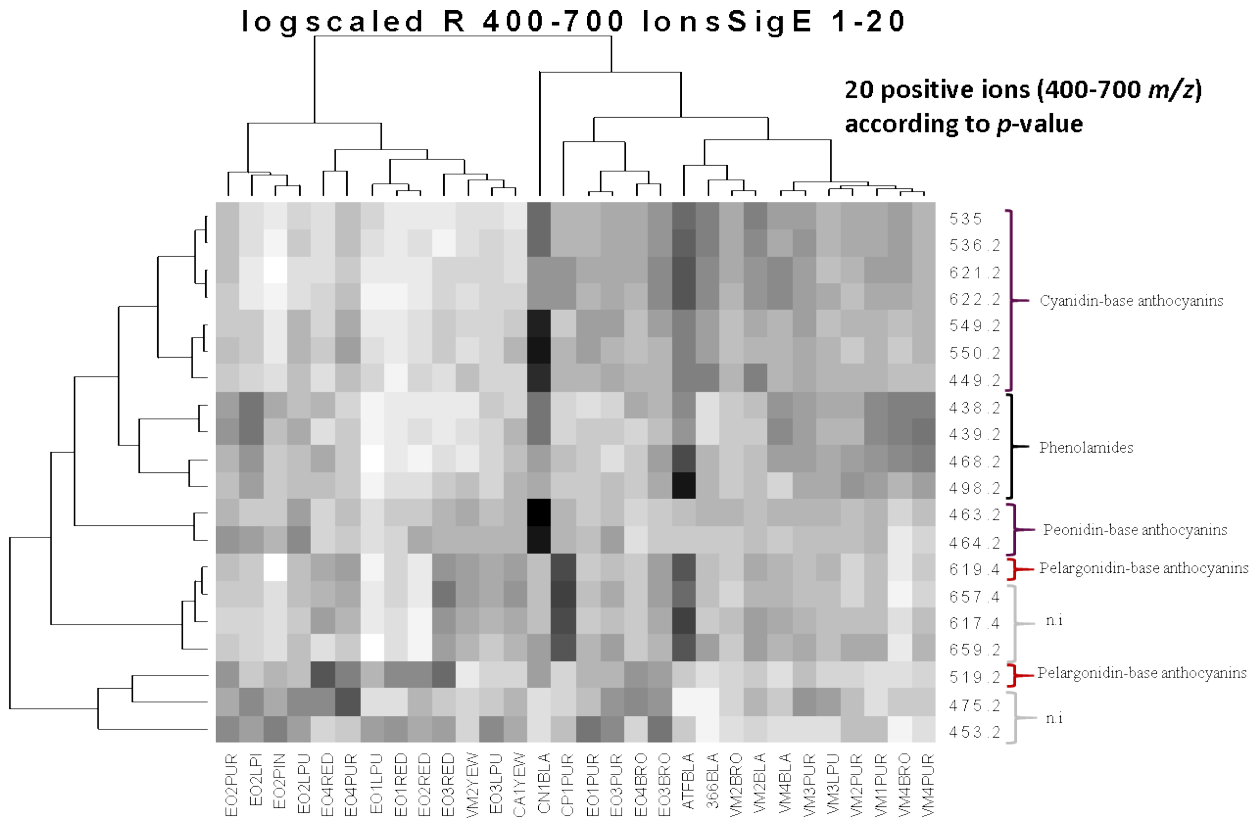

Figure S12. Heatmap using the most significant ions according to their p-value for the entry factor in the ANOVA model. The hierarchical clustering was done selecting the first 20 ions in the range from 400-700 m/z, which formed two clusters: one with higher anthocyanin concentration which included Vitamaize and brown colored kernels from “Elote occidental” purple grain from “Pozolero purpura”, and “Conico negro”. The second cluster grouped the rest: pale, red and purple colored genotypes.

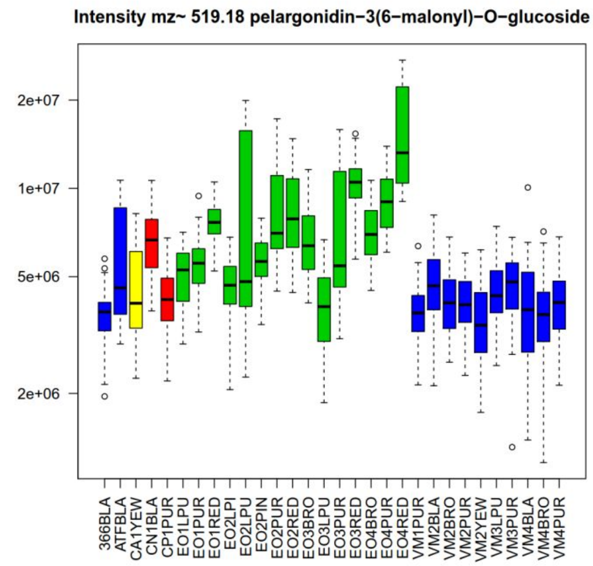

Figure S13. Boxplot distribution for pelargonidin-3-*O*-(6”-malonyl-glucoside) among different maize genotypes. It shows higher signal intensities for the “Elote Occidental” landrace in comparison to the other genotypes. The rectangles represent the first and third quartiles (boxes) and the median value (midline). The bars indicate the minimum and maximum values, whereas empty points represent data outliers.

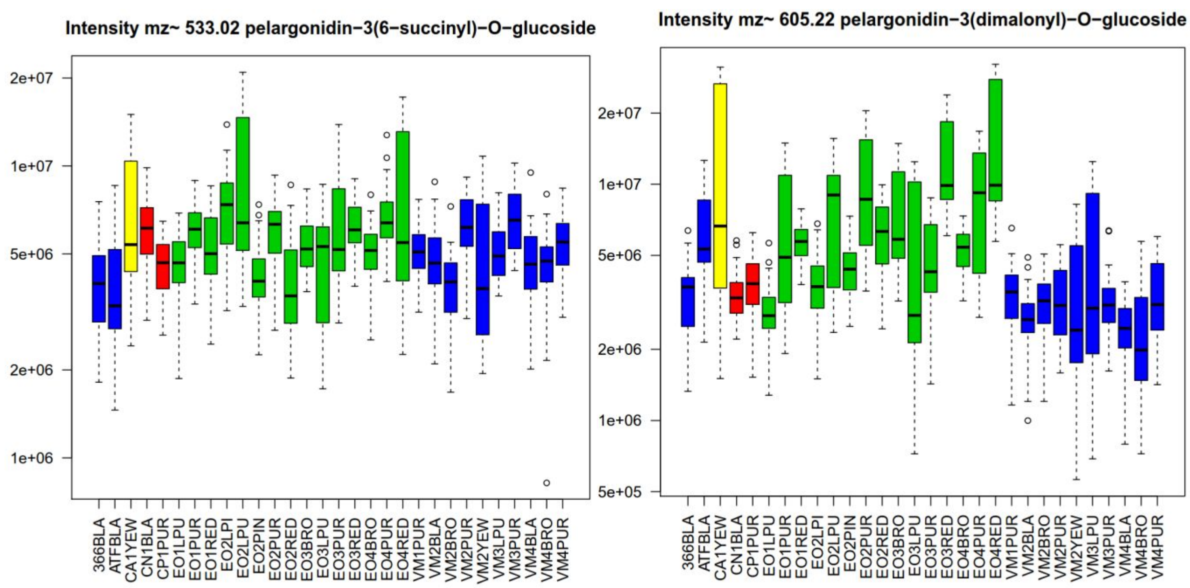

Figure S14. Boxplot distribution for ions corresponding to pelargonidin-3-*O*-(6”-succinyl-glucoside) and pelargonidin-3-*O*-(dimalonyl-glucoside).

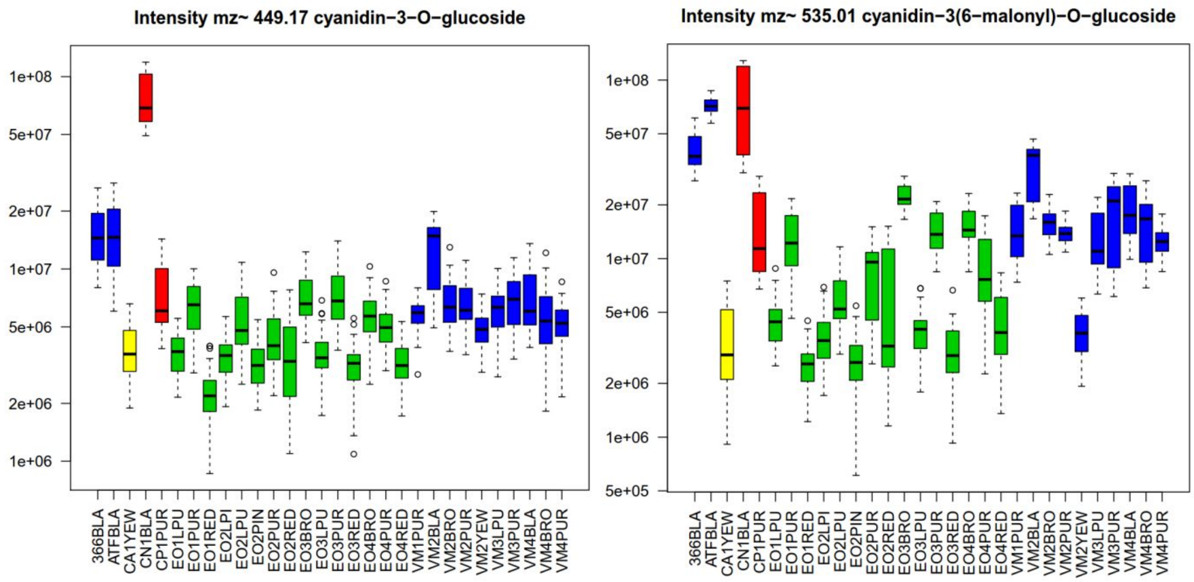

Figure S15. Boxplot distribution for ions corresponding to cyanidin-3-*O*-glucoside and cyanidin-3-*O*-(6”-malonyl-glucoside). Higher intensities correspond to kernel colors black, purple, and brown but Ven greater in CN1_Bla and vitamaize lines 366_Bla and ATF_Bla. Red and pale color kernels presented the lowest intensities.

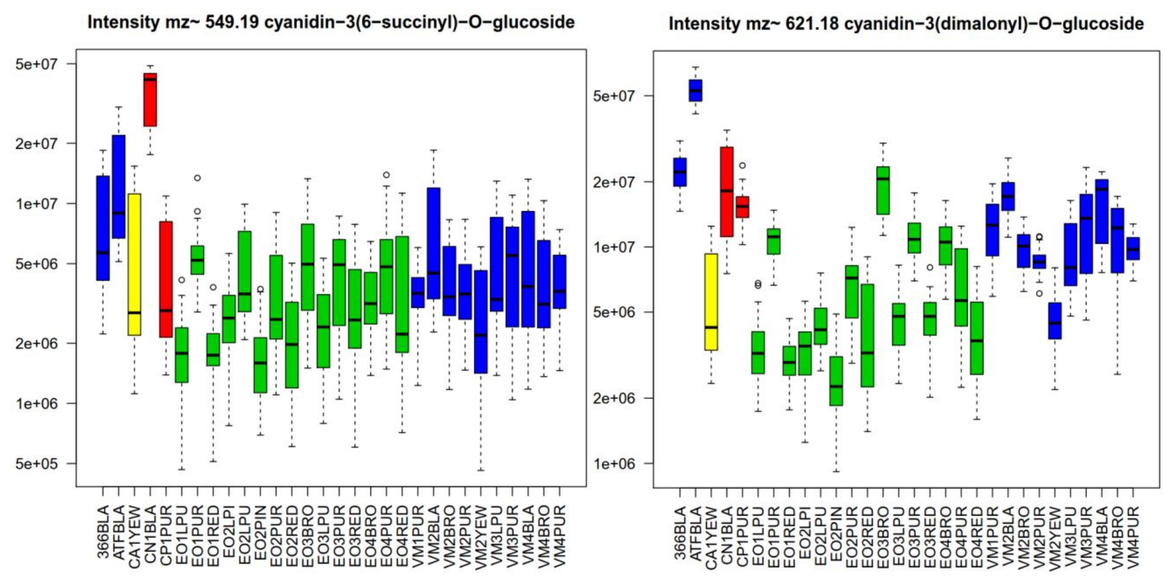

Figure S16. Boxplots distribution for cyanidin-3-*O*-(6”-succinyl-glucoside) and cyanidin-3-*O*-(dimalonyl-glucoside). These boxplots shown that higher intensities in both ions correspond to kernel colors black, purple, and brown but Ven greater in CN1_Bla and vitamaize lines as 366_Bla and ATF_Bla. Red and pale color kernels presented lower intensities.

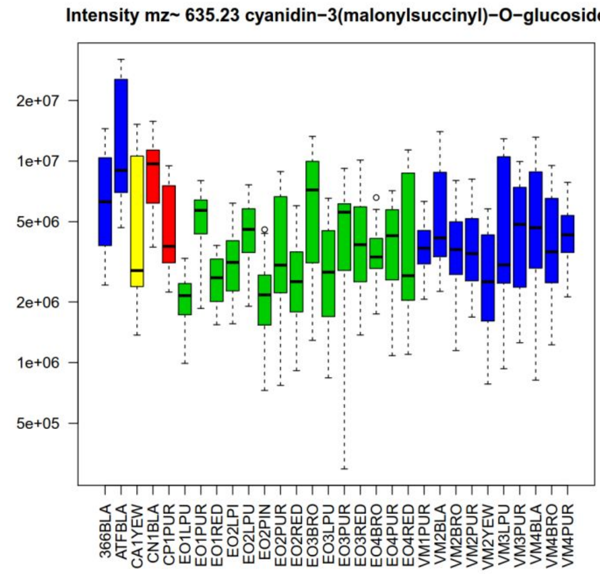

Figure S17. Boxplot distribution for cyanidin-3-*O*-(malonyl-succinyl)-glucoside. The ion had greater intensities in kernel colors like black, purple, and brown but Ven greater in CN1_Bla and vitamaize lines as 366_Bla and ATF_Bla. Red and pale color kernels presented the lower intensities.

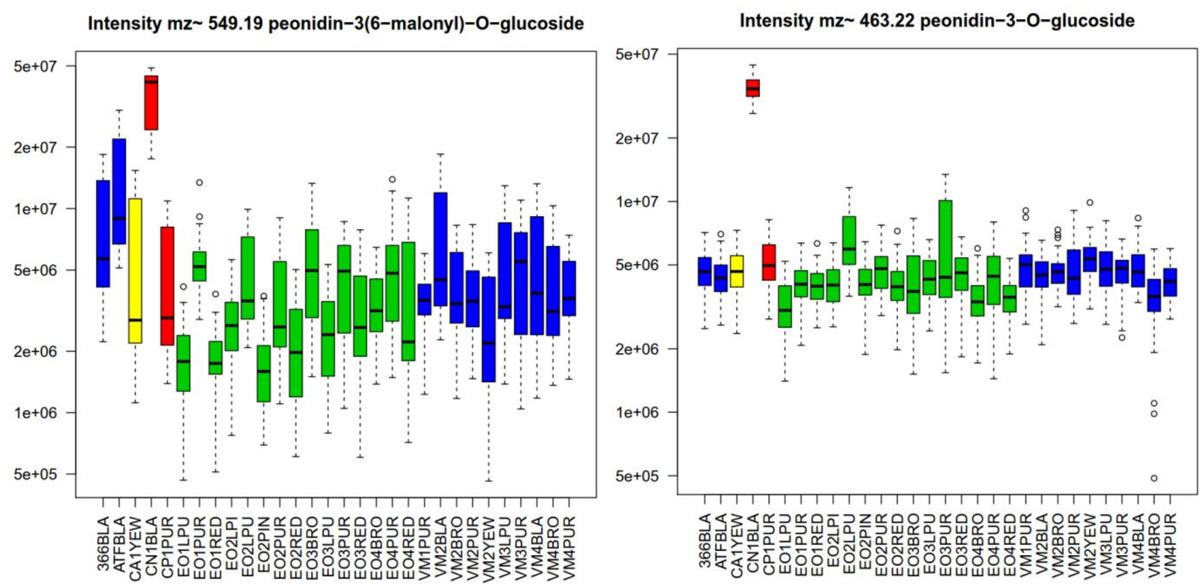

Figure S18. Boxplots for peonidin-3-*O*-(6"-malonyl-glucoside) and peonidin-3-*O*-glucoside. Both ions were highest in the CN1_Bla genotype.